

# The development of a 3D risk analysis method

Yet-Pole I<sup>\*</sup>, Te-Lung Cheng

*Department of Safety, Health, and Environmental Engineering, National Yunlin  
University of Science and Technology, Touliu 640, Taiwan*

Received 16 April 2007; received in revised form 15 August 2007; accepted 3 September 2007

Available online 5 September 2007

## Abstract

Much attention has been paid to the quantitative risk analysis (QRA) research in recent years due to more and more severe disasters that have happened in the process industries. Owing to its calculation complexity, very few software, such as SAFETI, can really make the risk presentation meet the practice requirements. However, the traditional risk presentation method, like the individual risk contour in SAFETI, is mainly based on the consequence analysis results of dispersion modeling, which usually assumes that the vapor cloud disperses over a constant ground roughness on a flat terrain with no obstructions and concentration fluctuations, which is quite different from the real situations of a chemical process plant. All these models usually over-predict the hazardous regions in order to maintain their conservativeness, which also increases the uncertainty of the simulation results. On the other hand, a more rigorous model such as the computational fluid dynamics (CFD) model can resolve the previous limitations; however, it cannot resolve the complexity of risk calculations. In this research, a conceptual three-dimensional (3D) risk calculation method was proposed via the combination of results of a series of CFD simulations with some post-processing procedures to obtain the 3D individual risk iso-surfaces. It is believed that such technique will not only be limited to risk analysis at ground level, but also be extended into aerial, submarine, or space risk analyses in the near future.

© 2007 Elsevier B.V. All rights reserved.

**Keywords:** 3D risk analysis; Maximum physical effects; Iso-surface; CFD; Storage tank; LPG

## 1. Introduction

Due to the increasing scale and complexity of a plant, the disasters of the chemical process industries become more and more severe during the past decades. Lots of efforts have been made in order to decrease the scale and possibility of chemical accidents. Quantitative risk analysis (QRA) [1–3] methodology that was originally used in aerospace, electronics, and nuclear power industries has also been employed in the chemical process industries. Many recent regulations, such as the Risk Management Program of the USA and the SEVESO II Directive of the EU, all include part or most of the QRA techniques in order to predict the severity or the possibility of potential hazards. Common QRA techniques, which include hazard identification, consequence analysis, frequency analysis, and risk calculation elements, are part of a risk management procedure (see Fig. 1).

By comparing the calculated individual risk profile and societal risk curve with some risk criteria, one can decide whether the risk is acceptable or whether engineering/management improvements are needed to reduce the risk to its target value. There are many new application and development of risk analysis technique during the past decade [4–11]. However, these risk analysis approaches can only predict the risk value of certain facilities and personnel in a two-dimensional format; it cannot differentiate the risk values of different level heights at the same location.

In order to improve this drawback, a 3D risk analysis technique was developed in this research and was applied to a series of fire and explosion simulations at the tank area within a petrochemical plant. This research employed the CFD software [12–14] to investigate the influence of three factors (overpressure, impulse pressure, and thermal radiation) that had hazardous effects on a spherical tank rupture accident. By applying the self-developed risk analysis module to adopt the simulation results from CFD, the 3D individual risk value can be estimated based on the results of these three factors.

<sup>\*</sup> Corresponding author. Tel.: +886 5 5342601x4493/4496/4421; fax: +886 5 5312069.

E-mail address: [iyp@yuntech.edu.tw](mailto:iyp@yuntech.edu.tw) (Y.-P. I).

### Nomenclature

A1–A4	floating-top tanks
B1–B4	floating-top tanks
D1–D2	refrigerated tanks
E1–E2	waste oil tanks
$F_1$ or $P$	overpressure (barg)
$F_2$ or $J$	pressure impulse (Pa s)
$F_3$ or $I$	thermal radiation (kW/m <sup>2</sup> )
$F_I$	incident frequency (1/year)
$F_i$	different physical parameters
$F_{i, \max}$	maximum physical effects
G1–G4	high-pressure spherical LPG tanks
I1–I3	ignition point
IR	individual risk (person/year)
$i$	index of hazardous physical effects
$I$	transient thermal radiation at a certain time and location (kW/m <sup>2</sup> )
$K_{i,1}, K_{i,2}$	conversion factors of the corresponding physical effects
$n$	number of hazardous physical effects
$P_I$	ignition probability of the released cloud
$P_{Di}$	personnel death percentages (%)
$P_{WIND}$	probability of eight different wind directions
$P_Z$	personnel appearance probability
$T$	radiation temperature (K)
$T_a$	initial ambient temperature (K)
$t$	time (s)
$t_e$	radiation elapse time interval (s)
$X_{HI}$	boundary plane at X-axis (with the highest coordinate value)
$X_{LO}$	boundary plane at X-axis (with the lowest coordinate value)
$(x, y, z)$	Cartesian coordinate
$Y_i$	personnel casualty probit values
$Y_{HI}$	boundary plane at Y-axis (with the highest coordinate value)
$Y_{LO}$	boundary plane at Y-axis (with the lowest coordinate value)
$Z_{HI}$	boundary plane at Z-axis (with the highest coordinate value)
$Z_{LO}$	boundary plane at Z-axis (with the lowest coordinate value)

## 2. Research method

### 2.1. Physical model

A physical model is used to predict different hazard severities and their possible ranges when enumerated incidents happen within a simulation site. In this study, a fire and explosion CFD software called FLACS [15–17] was employed as the physical model to simulate the “physical parameters of the fluid field” (overpressure, impulse pressure, temperature, and ventilation velocity, etc.) of the simulation site. FLACS is composed of

three parts: (1) CASD, which can build a 3D model of the simulation site and set different parameters used for simulation; (2) Flacs, which is the core program used for the 3D numerical simulation; and (3) Flow Vis, which is a post-processing module that can transform the simulation results into any 2D/3D format that can be observed from any angle or any cross-sectional plane. With its 3D dynamic characteristics, FLACS can facilitate the understanding of the spatial and transient distribution of many physical parameters that cannot be easily observed by traditional simulations.

### 2.2. Effect model

An effect model can adopt the simulation results from a physical model. It can evaluate the degrees of personnel casualty or facility damage affected by overpressure, pressure impulse, or thermal radiation. In this research, the effect model was constructed by the Compaq Visual Fortran 6.6 programming language and the METFOR 3.0 Fortran 90/95 Library. Necessary data was accessed from the FLACS output files in order to calculate the fire and explosion effects, and the final results were displayed via a series of 3D death percentage diagrams. In order to predict the hazard effective level of the simulation site, the “maximum physical effects” in each specific coordinate  $(x, y, z)$  within the hazard elapse time periods were proposed in this research. Different physical parameters  $(F_i(t, x, y, z))$ , which are a function of time and the Cartesian coordinate) were accessed from the FLACS output files by the effect model and then processed and saved as time independent “maximum physical effects  $(F_{i, \max}(x, y, z))$ ” according to Eq. (1), where  $F_1$ ,  $F_2$ , and  $F_3$  stand for overpressure ( $P$ ), pressure impulse ( $J$ ), and thermal radiation ( $I$ ), respectively; the transient thermal radiation at a certain time and location,  $I(t, x, y, z)$ , is calculated by the radiation elapse time interval  $(t_e(t, x, y, z))$ , initial ambient temperature ( $T_a$ ), and the radiation temperature  $(T(t, x, y, z))$  according to Eq. (2). First the “maximum physical effects” are converted into “personnel casualty probit values”  $(Y_i(x, y, z))$  according to Eq. (3), where  $K_{i,1}$  and  $K_{i,2}$  represent the conversion factors of the physical effects, and their corresponding values are shown in Table 1. Later the probit values are converted into “personnel death percentages”  $(P_{Di}(x, y, z))$  that are used for calculating the death toll within certain hazard incidents (see Eq. (4)).

$$F_{i, \max}(x, y, z) = \text{Max}_{t=1,2,\dots,n} F_i(t, x, y, z) \quad (1)$$

$$I(t, x, y, z) = 10^{-4} t_e(t, x, y, z) \{5.67 \times 10^{-8} [T^4(t, x, y, z) - T_a^4]\}^{4/3} \quad (2)$$

$$Y_i(x, y, z) = K_{i,1} + K_{i,2} \ln[F_{i, \max}(x, y, z)] \quad (3)$$

$$P_{Di}(x, y, z) = \frac{1}{(2\pi)^{1/2}} \int_{-\infty}^{Y_i(x, y, z)} \exp\left(-\frac{u^2}{2}\right) du \quad (4)$$

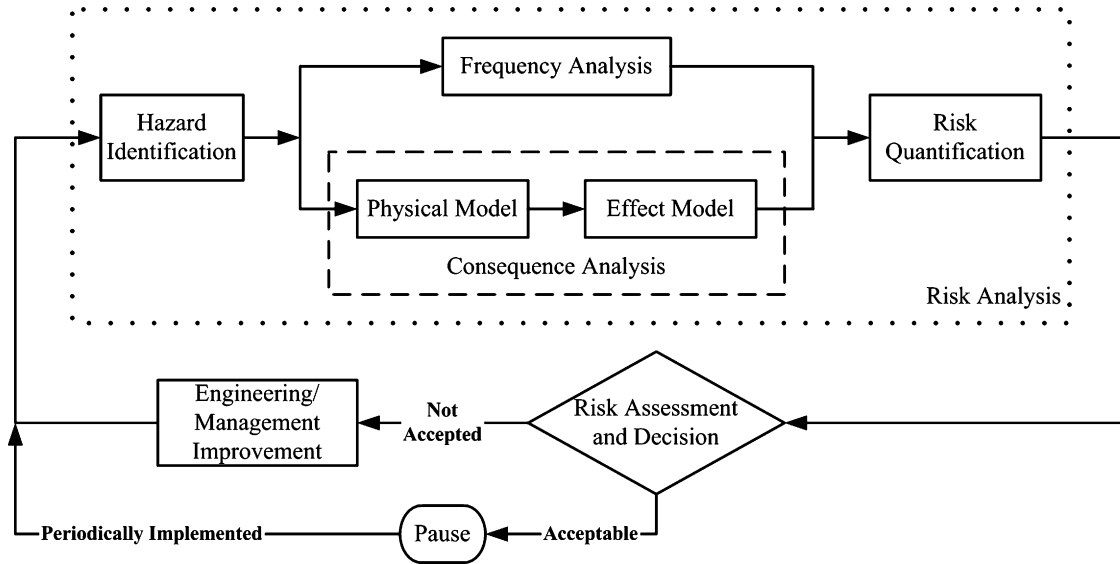


Fig. 1. Different risk analysis elements within a risk management procedure.

Table 1  
Probit formula for evaluating probit value [3,18] affected by different physical parameters

Physical parameter	Probit formula
Overpressure	$Y_1(x, y, z) = -77.1 + 6.91 \ln[P_{\max}(x, y, z)]$
Pressure impulse	$Y_2(x, y, z) = -46.1 + 4.82 \ln[J_{\max}(x, y, z)]$
Thermal radiation	$Y_3(x, y, z) = -14.9 + 2.56 \ln[I_{\max}(x, y, z)]$

2.3. Risk quantification

The purpose of individual risk analysis is to predict the yearly death rate of employees within a plant that has been influenced by certain hazard incidents (a fire and explosion incident was chosen in this research). The results of the effect model can be utilized to calculate the 3D death percentage; the latter can further be applied to predict each individual risks by combin-

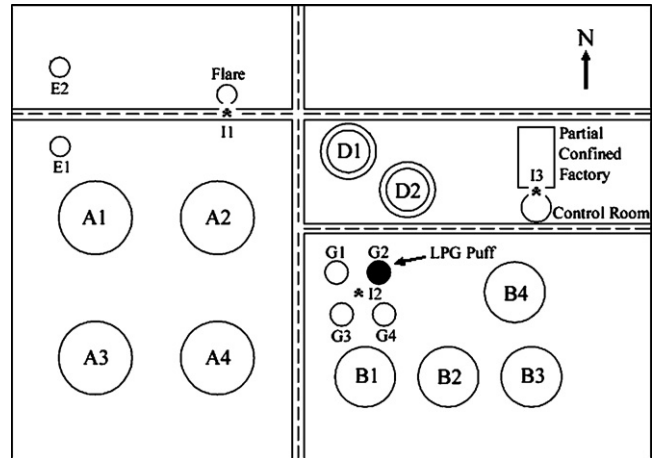


Fig. 2. Equipment layout for the simulation site; symbol “\*” stands for ignition point.

Table 2  
Wind-rose data at the simulation site

Wind(m/s)	N	NE	E	SE	S	SW	W	NW
< 1.0	0.04	0.04	0.021	0.008	0.01	0.01	0.010	0.017
1.0 - 2.0	0.09	0.07	0.038	0.011	0.02	0.02	0.030	0.045
2.0 - 3.0	0.06	0.02	0.008	0.009	0.03	0.02	0.044	0.051
3.0 - 4.0	0.03	0.00	0.002	0.007	0.02	0.01	0.036	0.043
4.0 - 5.0	0.01	0.00	0.000	0.004	0.01	0.00	0.016	0.028
5.0 - 6.0	0.00	0.00	0.000	0.002	0.01	0.00	0.007	0.012
6.0 - 7.0	0.00	0.00	0.000	0.001	0.00	0.00	0.002	0.005
7.0 - 8.0	0.00	0.00	0.000	0.000	0.00	0.00	0.001	0.002
SUM	0.23	0.13	0.07	0.04	0.10	0.06	0.15	0.20

Table 3  
Population distribution and its appearance probability of the simulation site

Location	Number of person (1)	Probability of appearance (2)	(1) × (2)
Vacant lots	6	0.1	0.6
Site roads	10	0.5	5
Tanks	2 × 16	0.2	6.4
Factory	8	1	8
Control room	15	1	15
Nominal total person	71	Real total of persons on site	35

ing the atmospheric environmental conditions, released cloud ignition rate, and incident frequency. The calculation algorithm for an individual risk is a revised form from Considine [1,2] as shown in Eq. (5), where IR(x, y, z) stands for the individual risk at a specific location; *i* and *n* stand, respectively, for the index and the number of hazardous physical effects (for overpressure, pressure impulse, and thermal radiation; *n* equals 3); *F<sub>I</sub>* stands for incident frequency (1 × 10<sup>-7</sup>/year was chosen in this study); *P<sub>I</sub>* stands for ignition probability of the released cloud (1 was chosen to represent a 100% ignition); *P<sub>WIND</sub>* represents probability of eight different wind directions (see Table 2; in order to simplify the calculation, the largest values (shaded blocks) from columns 2–9 were used to pick the “representing wind speeds” (shaded blocks in column 1) and the values on the bottom line (shaded blocks) were used as the “corresponding wind probabilities”); *P<sub>Z</sub>*(x, y, z) and *P<sub>Di</sub>*(x, y, z) represent the personnel appearance probability and death percentage, respectively, both of them belong to the function of coordinates. The total individual risk is the cumulative summation of risk values under different hazardous physical effects from certain enumerated incidents. The final result is displayed in a 3D iso-surfaces form and superimposed on a 3D plant facilities layout to facilitate the understanding by related personnel.

$$IR(x, y, z) = \sum_{i=1}^n F_I P_I P_{WIND} P_Z(x, y, z) P_{Di}(x, y, z) \quad (5)$$

Table 4  
The initial and boundary conditions used in FLACS simulations

Initial conditions		
Item	Unit	Value
Gravity constant	g/s <sup>2</sup>	9.8
Characteristic velocity	m/s	1.5 <sup>a</sup>
Relative turbulence intensity	–	0.05
Turbulence length scale	m	0.6
Temperature	°C	25
Ambient pressure	Pa	101,325
Ground height	m	0
Ground roughness	m	0.1
Reference height	m	11
Latitude	degree	23.5
Pasquill class	–	F
Ground roughness condition	–	Rural
Boundary conditions		
Item	Setting	Contents
<i>Y<sub>LO</sub></i> , <i>Y<sub>HI</sub></i> , <i>X<sub>LO</sub></i>	WIND	Speed = 1.5 <sup>a</sup> m/s, direction = from east <sup>a</sup> , buildup time = 0 s
<i>Z<sub>LO</sub></i>	WIND	Speed = 0 m/s
<i>X<sub>HI</sub></i> , <i>Z<sub>HI</sub></i>	PLANE WAVE	–

<sup>a</sup> The wind speed and directions of different simulations will be adjusted according to the shading areas of Table 2.

2.4. Description of the simulation site

A storage tank area (460 m long and 310 m wide) with a semi-confined factory, a control room, and a flare in a petrochemical plant was chosen as the simulation site in this research. There are three 8 m wide roads across the site and 16 tanks located at different areas (see Fig. 2), which include four 45,000 m<sup>3</sup> floating-top tanks (No. A1–A4), four 15,000 m<sup>3</sup> floating-top tanks (No. B1–B4), two 25,000 m<sup>3</sup> refrigerated tanks (No. D1–D2), four 2500 m<sup>3</sup> high-pressure spherical LPG tanks (No. G1–G4), and two smaller waste oil tanks (No. E1–E2). The cylindrical control

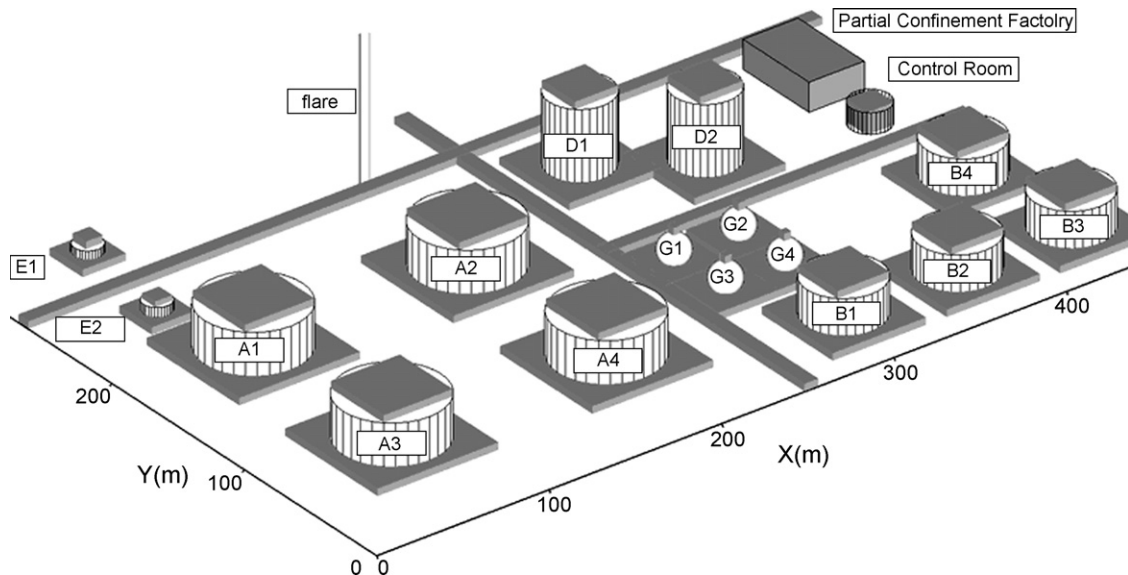


Fig. 3. 3D population distribution and equipment layout of the simulation site (shaded area).

room is in charge of controlling the transfer and dispensation of chemicals; the flare is responsible for handling the emergency discharged chemicals from the tank relief valves.

Usually the population distribution will directly influence the result of a risk analysis; therefore, it is necessary to investigate the on-site employee number and the corresponding appearance probability ( $P_Z$ ). The manpower deployment in a chemical process facility mainly depends on the employees' jobs and the characteristics of their activities. In addition, people will not always stay at the same place all day long unless the work is

extremely important; therefore, different shifts will take turns to keep the work/process uninterrupted. In this research, the control room and the factory is the most manpower-concentrated area, which have 15 and 8 persons, respectively, stay on their jobs 24 h a day. On the contrary, only six persons are spread out on various large vacant lots, and their individual  $P_Z$  value was set as 0.1 (see Table 3). Since people and cars must use the site roads to finish all kinds of activities, 10 persons are assigned on these roads and their  $P_Z$  value equals 0.5. It is assumed, in this study, that each tank has to be checked via a walk-

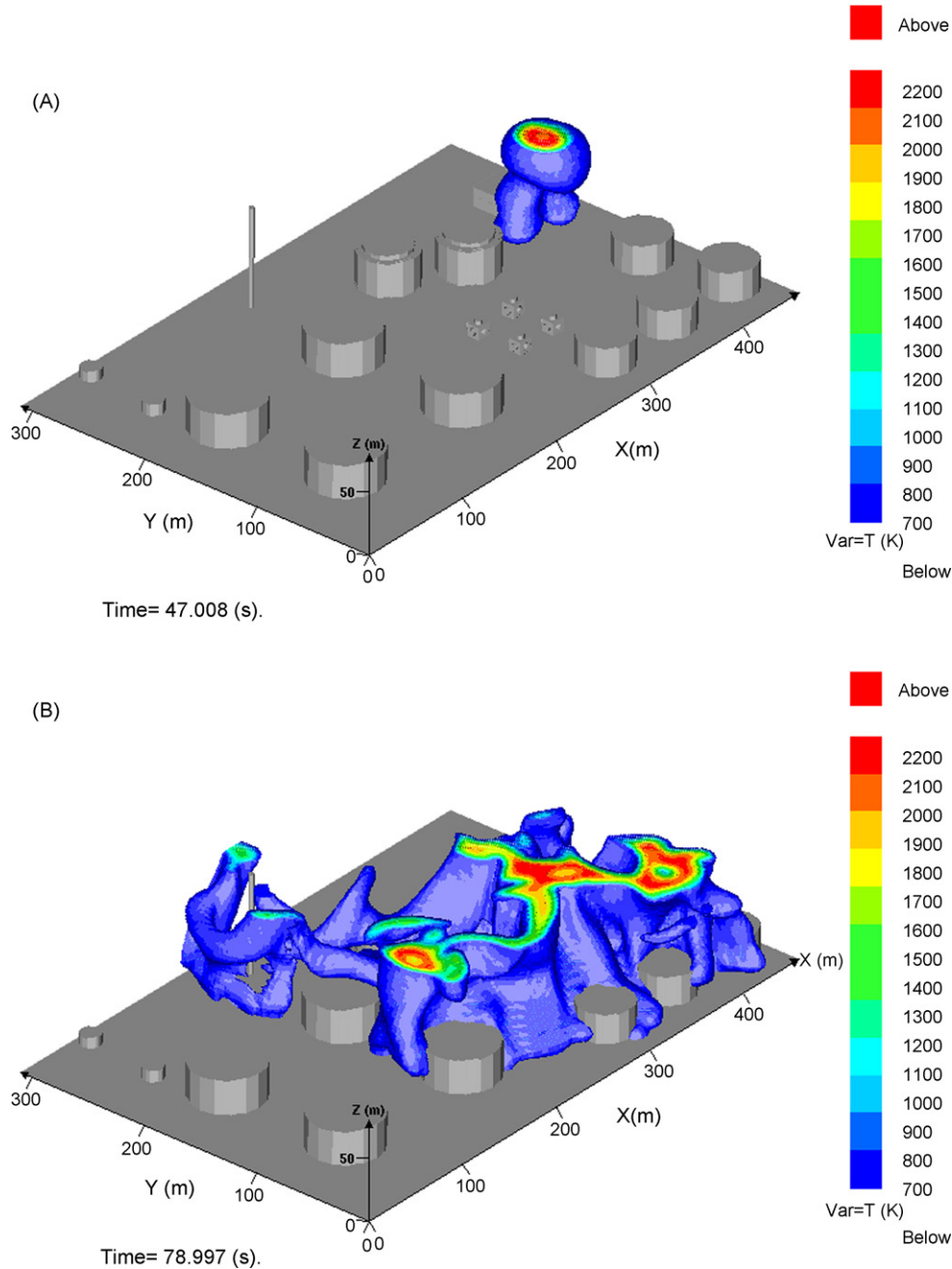


Fig. 4. High-temperature simulation consequence and its related calculation effects: (a) the flame-front progression (47 s); (b) the flame-front progression (79 s); (c) temperature iso-surfaces (700, 1273, and 1573 K) of the maximum temperature effect; (d) iso-surfaces of the personnel death percentage (1, 50, and 100%); (e) individual risk of thermal radiation under the east wind condition (3D View); (f) individual risk of thermal radiation under the east wind condition (projective view of X–Y plane).

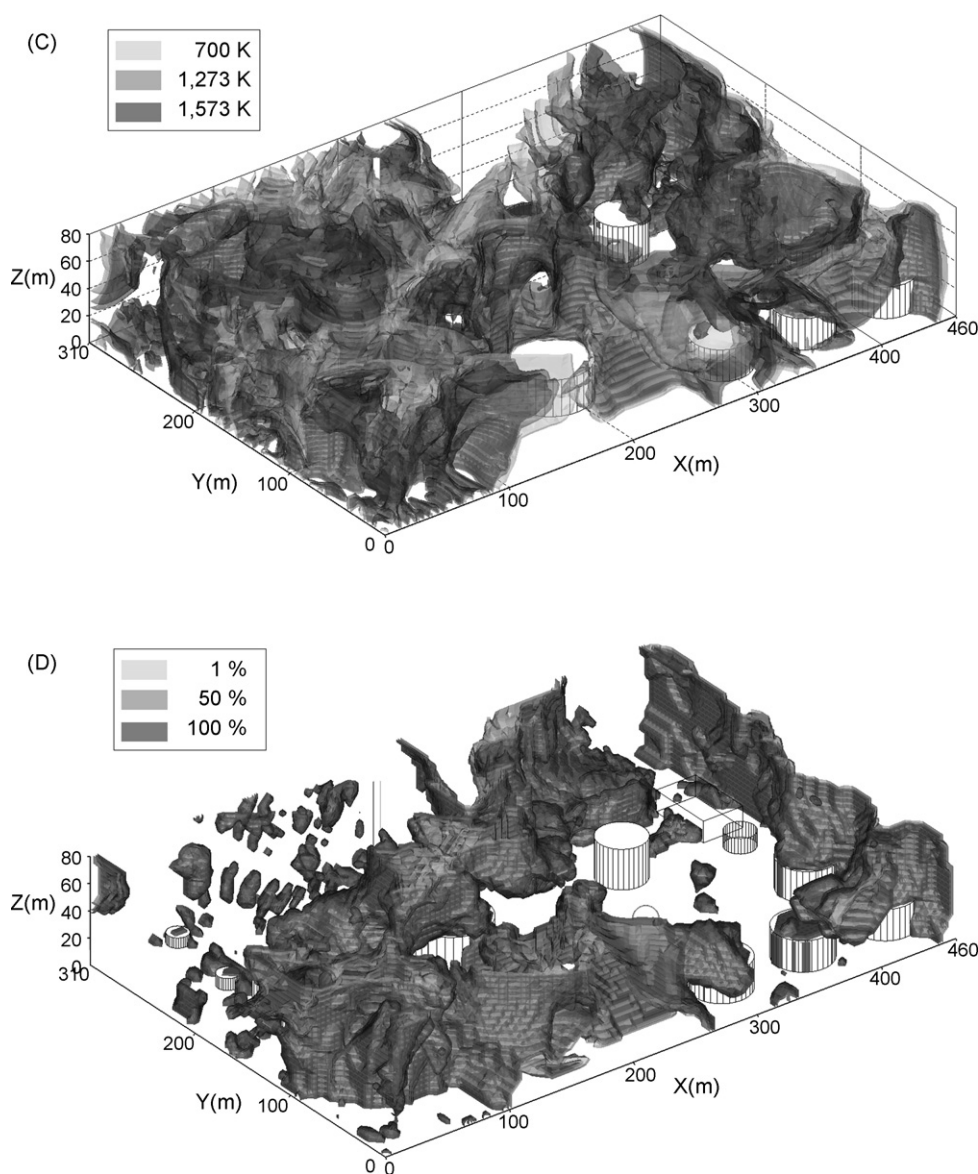


Fig. 4. (Continued).

through inspection by an operator every hour ( $10/60=0.167$ ) and to be maintained by at least two specialists for a week per year ( $(1/50) \times (12/24) \times 2=0.02$ ); in average, two persons are assigned to do these jobs and their individual  $P_Z$  value was set as 0.2 ( $0.167+0.02=0.187 \approx 0.2$ ). Usually people working at the tank site will show up either at the top endplate of the tank or on the ground within the dike area (see the grey areas of Fig. 3, the 3D population distribution inside the simulation site). Table 3 also lists the ranking of the  $P_Z$  value from high to low as follows: control room  $\geq$  factory > site roads > tank surrounding area > vacant lots.

### 3. Results and discussion

Worst-case scenario (WCS) is commonly employed in a risk management program for analyzing the most severe hazard that might happen within a certain process area. In this research, a disastrous rupture of a G2 LPG pressurized tank (the dark

area in Fig. 2) was chosen as the case study. The incident frequency was set as  $1 \times 10^{-7}$ /year since such case rarely happens or is almost entirely impossible [1]. It is assumed that the G2 tank accidentally ruptured and a  $60 \text{ m}^3$  LPG puff was formed from the release; later the dispersed gas cloud encountered three continuous ignition points that were located beside the flare, high-pressure spherical tank, and semi-confined factory (see I1–I3 in Figs. 2 and 3). The initial and boundary conditions of the simulation are listed in Table 4 for further reference. Since there are eight wind directions/probabilities in this study and their results are quite lengthy, only the results of the east-wind scenario are demonstrated here.

#### 3.1. Thermal radiation

After the G2 tank ruptured, the LPG puff quickly expanded and was dispersed by the east wind. It was ignited 41 s later; the edge of the diluted gas cloud reached its flammable range

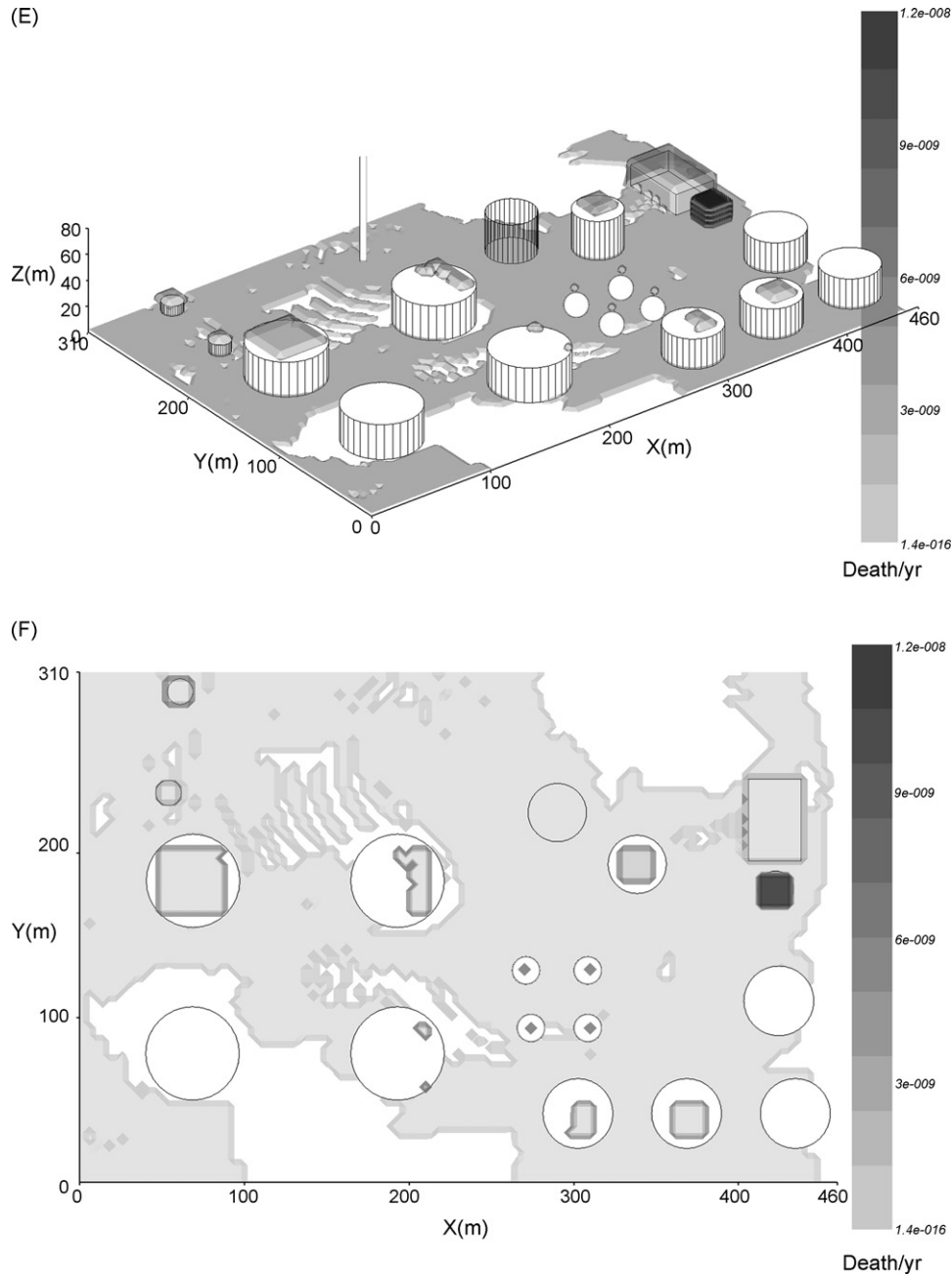


Fig. 4. (Continued).

and touched the ignition point I3. A deflagration phenomenon was observed, as a fireball was first formed and expanded at the south end of the semi-confined factory (see Fig. 4(A)). Since the flammable propane–air mixtures were spread all over the ground of the entire simulation site, the flame front made slow progress from the northeast end to the southwest end of the site (see Fig. 4(B)). It took about 50 s to burn off all the propane and the thermal radiation produced by the high temperature that seriously threatened the whole tank area. Fig. 4(C) shows that most of the tank area is covered by the temperature iso-surfaces above 1273 K, which will be fatal to the local personnel and will damage the equipment. According to Fig. 4(D), most of the site area is covered by the death percentage iso-surfaces that are

over 90%; together with the population distribution (see Fig. 3), the total casualty caused by thermal radiation can reach 31 persons. Fig. 4(E and F) shows the 3D and projective view of the individual risk arisen by thermal radiation under the east wind condition. It shows people in the control room possessed the highest individual risk ( $1.2 \times 10^{-8}$ ) in this disastrous accident since the population density there is also the highest. As for the vacant lots at the north side of the D2 tank and at the southwest side of the A4 tank, the individual risk values there are almost zero. The main reasons are (1) that the wind effect and blocking effect occurred by the presence of the D2 tank and the semi-confined factory, and (2) the population distribution there is also the lowest.

3.2. Pressure impulse

During the development of a large-scale deflagration period, the ambient pressure changed drastically; thus, the pressure impulse in the whole simulation area was almost larger than 18,000 Pa s, which will cause serious damage to the personnel and the equipment. According to the simulation results (not shown here), except for the top of tanks B1 and B3, almost all the plant’s ground areas were covered by the death percentage iso-surfaces that are higher than 90%. The death toll reached 21 persons under the influence of this physical effect.

3.3. Overpressure

According to the simulation results (not shown here), the overpressure values around the plant area for the G2 tank accident were all below 0.015 barg. This simulation result is suspiciously small [19]; however, for a medium reactivity, low obstacle density, and three-dimensional flame expansion, the value of even lower overpressure such as 0.01 barg (1 kPa) is possible for a soft ignition source [20]. Since such weak deflagration overpressure in an unconfined space will do limited harm to human beings, no death percentage zone or death toll was found in this case.

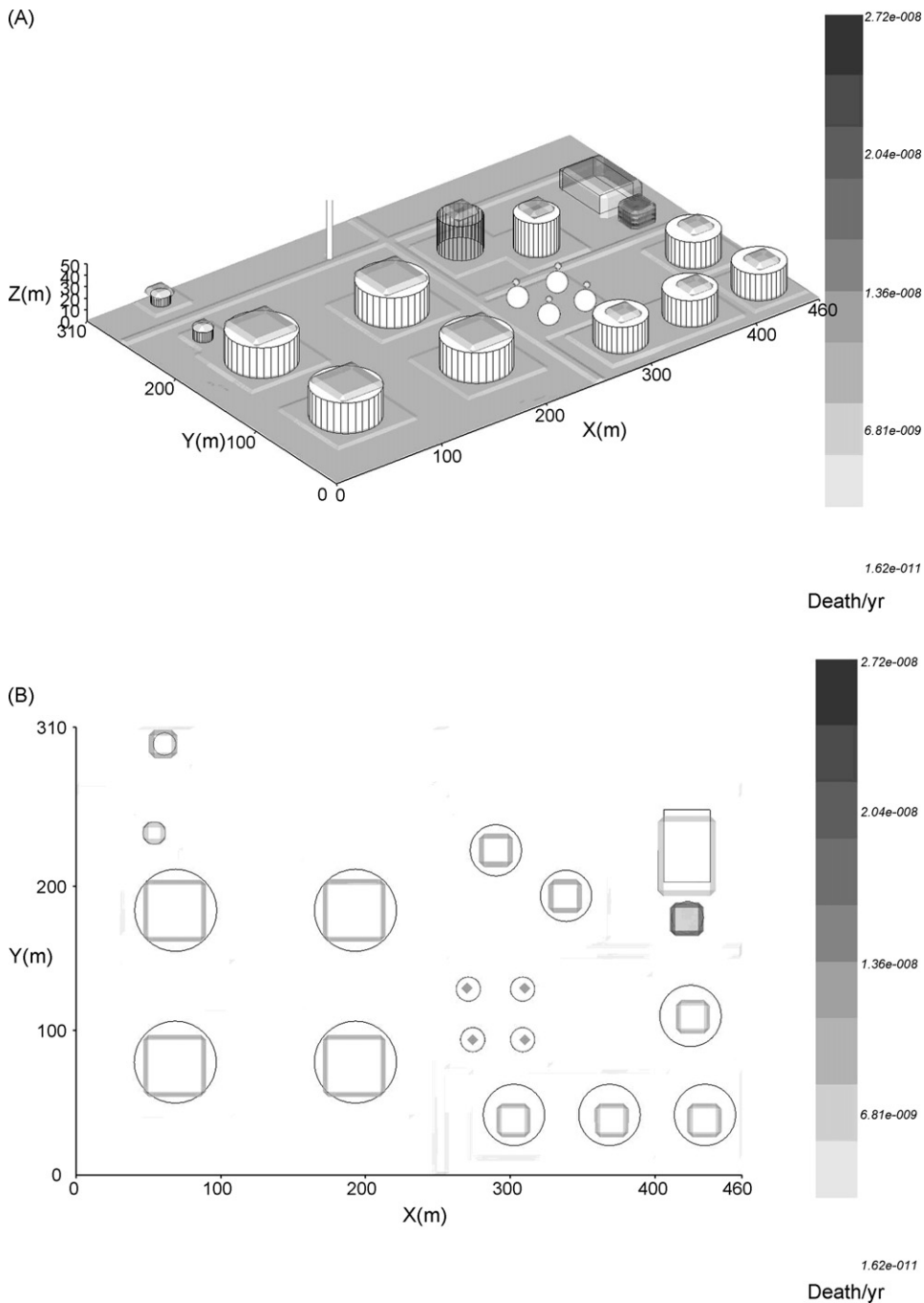


Fig. 5. Individual risk value for the G2 tank accident under the influence of the eight wind directions: (a) 3D view; (b) projective view of X–Y plane.

### 3.4. Total individual risk

Different individual risk values caused by thermal radiation, pressure impulse, and overpressure under the east wind scenario were added together; later, the risk values under the eight different wind scenarios were also accumulated in order to get the final 3D risk values (see Fig. 5). According to the simulation results, the ranking of the individual risk for the personnel located around the different facilities of the plant is (from high to low): control room ( $2.5 \times 10^{-8}$  person/year) > semi-confined factory ( $2.5 \times 10^{-9}$  person/year) > site roads ( $1.4 \times 10^{-9}$  person/year) > surroundings of tanks (from  $1.4 \times 10^{-9}$  to  $1.5 \times 10^{-10}$  person/year) > vacant sites ( $3.1 \times 10^{-11}$  person/year).

## 4. Conclusion

In this research, a self-developed risk calculation module and a fire and explosion CFD model that can consider the obstacle effects were combined to implement the risk analysis task for a petrochemical tank area. The proposed 3D risk analysis technique can expand beyond the limitation of the traditional methods that can only predict the risk value on the ground. Unlike the traditional methods that average many environmental influences (the terrain effect, the obstacle effect, and concentration fluctuations, etc.), the new method can also differentiate a more subtle risk difference in different spaces with the help of the CFD algorithm. A spherical tank rupture accident was chosen to investigate the influence of wind directions on the flammable concentration range, the ignition priority, the fire and explosion consequence, and the individual risk distribution. The simulation results showed that employees in the control room would receive the highest risk ( $2.5 \times 10^{-8}$  person/year), while the risk in the vacant lots would be the lowest ( $3.1 \times 10^{-11}$  person/year). The study also showed that an apparent risk difference exist between different heights at the same location. In conclusion, the 3D risk analysis technique proposed in this research cannot only be used in the chemical industry, but can also be extended to other industries where height (depth) is a critical factor. Therefore, it is foreseeable that different realistic applications can be greatly improved by using this method.

## Acknowledgements

The authors are grateful to the GexCon AS for providing the FLACS software and to the National Science Council of Taiwan for the financial support of this study under the project entitled “Development of a 3D risk analysis technique (NSC 94-2211-E-224-007-).”

## References

[1] F.P. Lees, Loss Prevention in the Process Industries, Butterworth, New York, 1996.

- [2] CCPS/AIChE, Guidelines for Chemical Process Quantitative Risk Analysis, Wiley, New York, 2000.
- [3] A.D. Crowl, J.F. Louvar, Chemical Process Safety: Fundamentals with Applications, Prentice Hall, Upper Saddle River, 2002.
- [4] F.I. Khan, S.A. Abbasi, Techniques and methodologies for risk analysis in chemical process industries, J. Loss Prev. Process Ind. 11 (1998) 261–277.
- [5] H. Frantzych, Risk analysis and fire safety engineering, Fire Safe. J. 31 (1998) 313–329.
- [6] P.H. Bottelberghs, Risk analysis and safety policy developments in the Netherlands, J. Hazard. Mater. 71 (2000) 59–84.
- [7] K. Oien, Risk indicators as a tool for risk control, Reliab. Eng. Sys. Safe. 74 (2001) 129–145.
- [8] E. Salzano, I. Iervolino, G. Fabbrocino, Seismic risk of atmospheric storage tanks in the framework of quantitative risk analysis, J. Loss Prev. Process Ind. 16 (2003) 403–409.
- [9] P.K. Roy, A. Bhatt, C. Rajagopal, Quantitative risk assessment for accidental release of titanium tetrachloride in a titanium sponge production plant, J. Hazard. Mater. A102 (2003) 167–186.
- [10] M. Demichela, N. Piccinini, A. Romano, Risk analysis as a basis for safety management system, J. Loss Prev. Process Ind. 17 (2004) 179–185.
- [11] F.J. Groen, C. Smidts, A. Mosleh, QRAS—the quantitative risk assessment system, Reliab. Eng. Sys. Safe. 91 (2006) 292–304.
- [12] D.D. Herrmann, Improved vapor cloud explosion predictions by combining CFD modeling with the Baker–Strehlow method, in: Proceeding of International Conference and Workshop on Modeling the Consequence of Accidental Releases of Hazardous Materials, San Francisco, USA, 1999, pp. 479–494.
- [13] S. Høiset, B.H. Hjertager, T. Solberg, K.A. Malo, Flixborough revisited—an explosion simulation approach, J. Hazard. Mater. 77 (2000) 1–9.
- [14] H.S. Ledin, C.J. Lea, A review of the state-of-the-art in gas explosion modelling, Fire and Explosion Group, UK (2002) HSL/2002/02 <http://www.hse.gov.uk/research/hsl.pdf/2002/hsl02-02.pdf>.
- [15] O.R. Hansen, O. Talberg, J.R. Bakke, CFD-based methodology for quantitative gas explosion risk assessment in congested process areas: examples and validation status, in: Proceeding of International Conference and Workshop on Modeling the Consequence of Accidental Releases of Hazardous Materials, San Francisco, USA, 1999, pp. 457–477.
- [16] S.R. Hanna, O.R. Hansen, S. Dharmavaram, FLACS air quality CFD model performance evaluation with Kit Fox, MUST, Prairie Grass, and EMU observations, J. Atmos. Environ. 38 (2004) 4675–4687.
- [17] S. Dharmavaram, S.R. Hanna, O.R. Hansen, Consequence analysis—using a CFD-model for industrial sites, Process Safe. Prog. 24 (2005) 316–327.
- [18] S. O’Sullivan, S. Jagger, Human vulnerability to thermal radiation offshore, Fire and Explosion Group, UK (2004) HSL/2004/04, <http://www.hse.gov.uk/research/hsl.pdf/2004/hsl04-04.pdf>.
- [19] J.S. Puttock, M.R. Yardley, T.M. Cresswell, Prediction of vapour cloud explosions using the SCOPE model, J. Loss Prev. Process Ind. 13 (2000) 419–431.
- [20] TNO, Method for the calculation of physical effects – due to the releases of hazardous materials (liquids and gases) – ‘Yellow Book’, CPR14E (Part 2), Directorate General for Social Affairs and Employment, The Hague, 1997. Also available as a software package (EFFECTS).

## Glossary

WCS: worst-case scenario

LPG: liquefied petroleum gas

CFD: computational fluid dynamics